Journal of Imaging Science and Technology® 53(6): 060403–060403-8, 2009.

Principal Component Analysis-Based Reflectance Analysis/ Synthesis of Cosmetic Foundation

Shoji Tominaga▲ and Yusuke Moriuchi
Department of Information Science, Graduate School of Advanced Integration Science, Chiba University, 1-33, Yayoi-cho, Inage-ku, Chiba 263-8522, Japan
E-mail: shoji@faculty.chiba-u.jp

Abstract. *This article analyzes the spectral reflection properties of skin surface with make-up foundation. Foundations with different material compositions are painted on a bioskin. First, the authors measure the spectral reflectance of the skin surfaces under a variety of conditions of light incidence and viewing. Second, the authors show the limitations of the model-based approach for describing the reflectance curves by a small number of parameters. A new approach based on the principal component analysis is then proposed for describing the detailed shape of the surface-spectral reflectance function. All skin surfaces exhibit the property of standard dichromatic reflection, so that the observed reflectances are expressed as a linear combination only two spectral components of a constant reflectance and a diffuse reflectance. Moreover, the authors find that the weighting coefficients are decomposed into two basis functions with a single parameter. As a result, the spectral reflectance under arbitrary observation conditions can be estimated by synthesis of the diffuse spectral reflectance and several one-dimensional basis functions. Finally, the feasibility of the proposed approach is examined in detail in experiments using real foundation samples. © 2009 Society for Imaging Science and Technology.*
[DOI: 10.2352/J.ImagingSci.Technol.2009.53.6.060403]

INTRODUCTION

The estimation of human skin color has been a popular topic in many fields, including color reproduction, image processing, computer graphics, medical imaging, and cosmetics development. There are recent research reports on the spectral analysis of skin color.[1–3]

Foundation is a cosmetic preparation which is applied to the skin to improve the appearance of the skin surface. It has various purposes. For instance, foundation makes skin color and skin texture appears more even. It can be used to cover up blemishes and other imperfections and reduce wrinkles. Therefore, it is important to evaluate the change in skin color by the foundation. However, to our knowledge, there is no scientific discussion on the spectral analysis of foundation material and skin with make-up in the visible range, only for the IR spectrum.[4]

The present article analyzes the spectral reflection properties of skin surface with make-up foundation. Foundations with different material compositions are painted on a bioskin. Surface-spectral reflectance of the skin surface is measured goniophotometrically. Appearances of the surface, including specularity, gloss, and matte appearance, depend on the observation conditions of light incidence and viewing and also the material compositions. First, we investigate a relationship between the surface reflectance and the various conditions of observation and material composition. Next, we show the limitations of the model-based approach used to describe the complicated reflectance curves using a small number of parameters.

We then consider a new approach to describe the detailed shape of the surface-spectral reflectance function of the skin with make-up foundation. First, we investigate the basic property of the skin surface based on the principal component analysis (PCA) of the whole set of spectral reflectances measured in the visible range under a variety of conditions of light incidence and viewing. We show that all the surfaces satisfy the property of standard dichromatic reflection, so that the observed reflectances can be represented by only two spectral components: a constant reflectance and a diffuse reflectance. Moreover, we analyze the weighting coefficients for the spectral components, depending on the incidence and viewing directions and find that the weighting coefficients can be decomposed into two basis functions using a single parameter. Thus, the spectral reflectance at arbitrary observation conditions can be estimated by synthesizing the diffuse spectral reflectance and several one-dimensional basis functions. Finally, the feasibility of the proposed method for reflectance estimation is examined using foundation samples with different material compositions. Color images of a skin surface are rendered using the estimated spectral reflectances.

FOUNDATION SAMPLES

The make-up foundation is composed of different materials such as mica, talc, nylon, titania, and oil. Two materials of mica and talc are the important components, which affect the appearance of skin surface painted with the foundation. Many different foundations were made by changing the quantity and the ratio of two materials. For instance, the combination ratio of mica (M) and talc (T) was changed as ($M=0$, $T=60$), ($M=10$, $T=50$),…, ($M=60$, $T=0$), and the ratio of mica was changed with a constant T as ($M=0$, $T=40$), ($M=10$, $T=40$),…, and ($M=40$, $T=40$). Thus, we have many combinations to produce a variety of foundations. Table I shows the foundation samples used for the spectral reflectance analysis in this study. Figure 1 shows

▲IS&T member.

Received Jan. 27, 2009; accepted for publication Jun. 24, 2009; published online Oct. 8, 2009.
1062-3701/2009/53(6)/060403/8/$20.00.

Table I. Foundation samples with different composition of mica and talc.

Samples	IKD-0	IKD-10	IKD-20	IKD-40	IKD-54	IKD-59
mica	0	10	20	40	54	59
talc	59	49	39	19	5	0

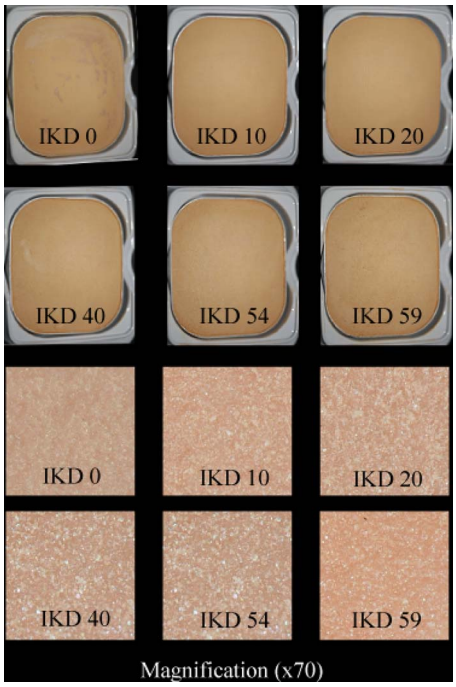

Figure 1. Group photo of the samples in foundation containers and the magnified surfaces.

Figure 2. Sample of bioskin with foundation.

a group photo of the samples in foundation containers and the magnified surfaces.

The bioskin used in this study is made of a urethane surface that looks like human skin. Powder foundations with the above compositions were painted on a flat bioskin surface with the fingers. Figure 2 shows a board sample of bioskin with foundation. The foundation layer is very thin, 5–10 μm in thickness on the skin.

REFLECTANCE MEASUREMENTS

A goniospectrophotometer was used for observing surface-spectral reflections of the skin surface with foundations under different lighting and viewing conditions. The measuring system has two degrees of freedom: light source position and

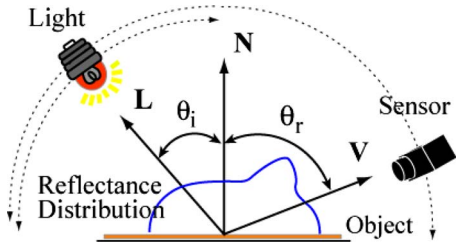

Figure 3. System of measuring surface reflectance.

the sensor position, as shown in Figure 3, where the vectors **N**, **L**, and **V** indicate, respectively, the normal direction of an object surface, the light source direction, and the sensor direction. Therefore, θ_i is the light incidence angle and θ_r is the viewing angle. In the real instrument (Murakami GCMS-4) we used, the sensor position is fixed, while both light source and sample object can rotate. The ratio of the spectral radiance from the sample to the one from the reference white diffuser called the spectral radiance factor is output as spectral reflectance.

The spectral reflectances of all samples were measured at 13 incidence angles of 0°, 5°, 10°,…,60° and 81 viewing angles of −80°, −78°, …,−2°, 0°, 2°,…,78°, 80°. Figure 4(a) shows a three-dimensional (3D) perspective view of spectral radiance factors measured from the bioskin itself and the skin with a foundation sample IKD-54 at the incidence angle of 20°. Red solid mesh and black solid mesh indicate the spectral radiance factors from IKD-54 and bioskin itself, respectively. This figure suggests how the foundation effectively changes the spectral reflectance of the skin surface. The spectral reflectance depends not only on the viewing angle but also on the incidence angle. In order to make this point clear, we average the radiance factors on wavelength in the visible range. Figure 4(b) depicts a set of the average curves at different incidence angles as a function of viewing angle for both IKD-54 and the bioskin.

A comparison between black solid curves and red solid curves in Fig. 3 suggests several typical features of skin surface reflectance with foundation. The three particular features are

(1) Reflectance maximum at around the vertical viewing angle,
(2) Back-scattering at around −70°, and
(3) Increasing specular reflectance with increasing viewing angle.

The same features are observed for the other samples (e.g., see Ref. 5 for IKD-20).

Moreover, we have investigated how the surface reflectance depends on the material composition of foundation.

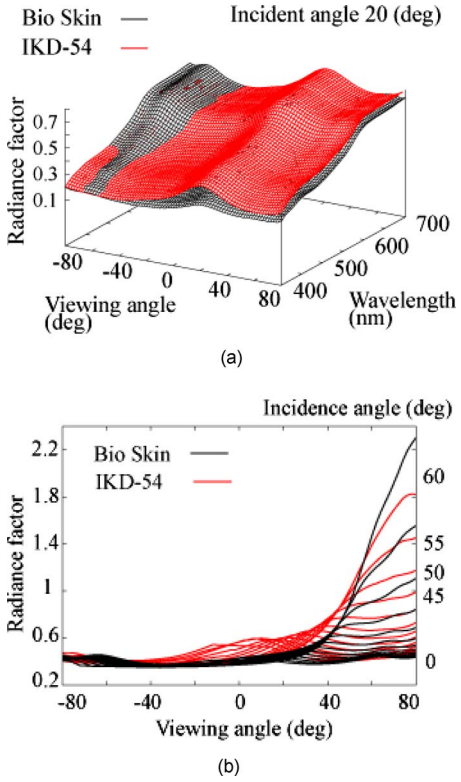

Figure 4. Reflectance measurements from sample IKD-54 and bioskin. (a) 3D view of spectral reflectances at $\theta_i = 20$. (b) Average reflectances as a function of viewing angle.

Figure 5 shows the average reflectances for three cases among difference material compositions. Two basic properties are found as follows:

(1) When the quantity of mica increases, the whole reflectance of skin surface increases at all incident angles and at viewing angles greater than 20°.
(2) When the quantity of talc increases, the surface reflectance decreases at large viewing angles while it increases at matte regions.

MODEL-BASED ANALYSIS

The Phong model[6] and the Cook-Torrance model[7] are known as 3D reflection models used for describing light reflection of an object surface. The former model is convenient for the description of inhomogeneous dielectric objects like plastics. The mathematical expression of the model is relatively simple, and the number of model parameters is small. The latter model is a physically precise model, which is available for both dielectrics and metals. Tominaga et al.[8] examined the two models for the description of 3D light reflection of oil painting surfaces. It was shown that the Cook-Torrance model could describe the reflection properties of oil paints more precisely than the Phong model. So we examine this model for foundation samples.

The Cook-Torrance model is written in terms of the spectral radiance factors as

$$Y(\lambda) = S(\lambda) + \beta \frac{D(\varphi,\gamma)G(\mathbf{N},\mathbf{V},\mathbf{L})F(\theta_Q,n)}{\cos\theta_i \cos\theta_r}, \qquad (1)$$

where the first and second terms represent, respectively, the diffuse and specular reflection components. The symbol β represents the specular reflection coefficient. A specular surface is assumed to be an isotropic collection of planar microscopic facets by Torrance and Sparrow.[9] The area of each microfacet is much smaller than the pixel size of an image. Note that the surface normal vector **N** represents the normal vector of a macroscopic surface. Let **Q** be the vector bisector of an **L** and **V** vector pair, that is, the normal vector of a microfacet. The symbol θ_i is the incidence angle, θ_r is the viewing angle, φ is the angle between **N** and **Q**, and θ_Q is the angle between **L** and **Q**.

The specular reflection component consists of several terms: D is the distribution function of the microfacet orientation, and F represents the Fresnel spectral reflectance[10] of the microfacets; G is the geometrical attenuation factor. We assume D to be a Gaussian distribution function with rotational symmetry about the surface normal **N** as

$$D(\varphi,\gamma) = \exp\{-\log(2)\varphi^2/\gamma^2\}, \qquad (2)$$

where the parameter γ is a constant that represents surface roughness. The Fresnel reflectance F is described as a nonlinear function with the parameter of the refractive index n (see Ref. 11).

The unknown parameters in this model are the coefficient β, the roughness γ, and the refractive index n. The reflection model is fitted to the measured spectral radiance factors by the method of least-squares. In the fitting computation, we used the average radiance factors on wavelength in

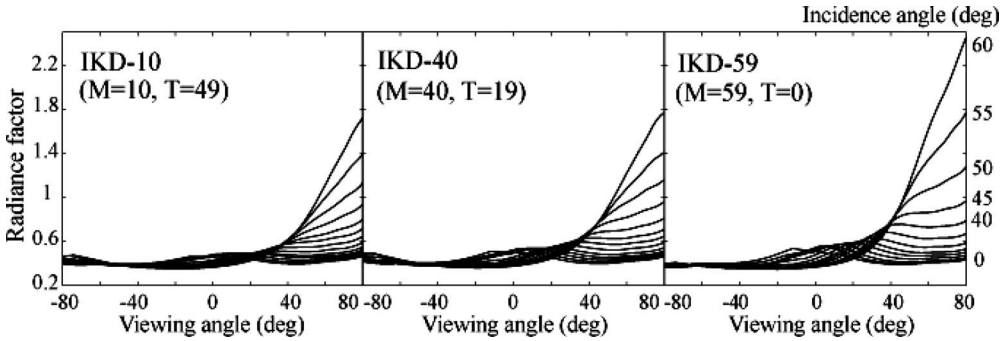

Figure 5. Reflectance measurements from different make-up foundations.

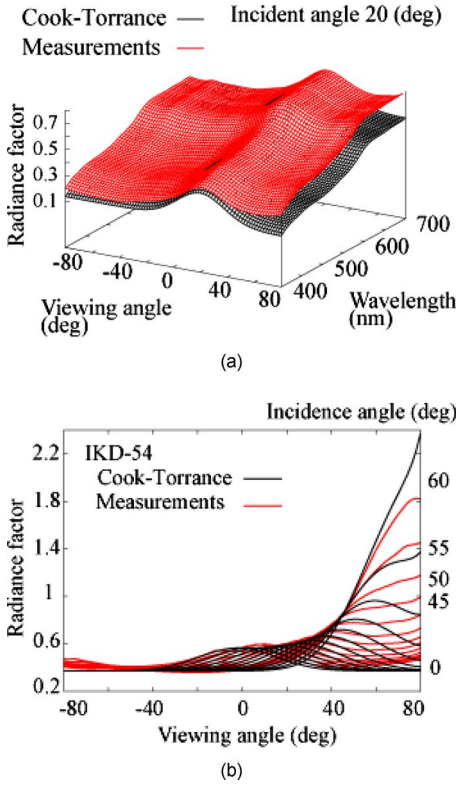

Figure 6. Fitting results of the Cook-Torrance model to IKD-54. (a) 3D view of spectral reflectances at $\theta_i = 20$. (b) Average reflectances as a function of viewing angle.

the visible range. We determine the optimal parameters to minimize the squared sum of the fitting error

$$e = \min \sum_{\theta_i, \theta_r} \left\{ \overline{Y(\lambda)} - \overline{S(\lambda)} - \beta \frac{D(\varphi, \gamma) G(\mathbf{N}, \mathbf{V}, \mathbf{L}) F(\theta_Q, n)}{\cos \theta_i \cos \theta_r} \right\}^2, \tag{3}$$

where $\overline{Y(\lambda)}$ and $\overline{S(\lambda)}$ are the average values of the measured and diffuse spectral reference factors, respectively. The diffuse reflectance $S(\lambda)$ is chosen as a minimum of the measured spectral reflectance factors without noise. For noisy observations, $S(\lambda)$ is determined from the average of the measured spectra with low radiance. The above error minimization is done over all angles of θ_i and θ_r. In this article, for simplicity of model fitting, we use the refractive index $n = 1.90$ of an inhomogeneous dielectric for the foundations.

Figure 6 shows the results of model fitting to the sample IKD-54 shown in Fig. 4, where black curves indicate the fitted reflectances and red curves indicate the original measurements. The model parameters were estimated as $\beta = 0.74$ and $\gamma = 0.17$. The squared error was $e = 6.56$. Figure 6(a) shows the 3D view of the fitting results for spectral reflectances at the incidence angle of 20°. These figures suggest that, although the model describes the surface reflectances at the low range of viewing angle with relatively good accuracy, the fitting error tends to increase with the viewing angle.

We have repeated the same fitting experiment of the model to the foundation samples with different material compositions. Table II shows a list of the estimated model parameters and the fitting errors for foundations IKD-0-IKD-59. The fitting results for these samples are similar to Fig. 6. A similar discrepancy to that seen with IKD-54 occurs between the estimated reflectances by the model and the direct measurements for all the other samples (e.g., see Ref. 5 for IKD-20). These results show the limitations of the model-based method for describing the complicated spectral reflectance curves using a small number of parameters.

Table II. Model parameters and the fitting errors for different foundations.

Samples	Parameters β	Parameters γ	Fitting errors e
IKD-0	0.431	0.249	2.45
IKD-10	0.426	0.249	2.62
IKD-20	0.485	0.220	4.11
IKD-40	0.570	0.191	4.79
IKD-54	0.744	0.170	6.56
IKD-59	0.736	0.180	4.44

PCA-BASED ANALYSIS/SYNTHESIS

We consider a new approach to estimate the detailed shape of the surface-spectral reflectance of the skin with make-up foundation using PCA.

Analysis

First, we investigate the basic reflection property of the skin surface. The standard dichromatic reflection model[12] assumes that the surface reflection consists of two additive components, the body (diffuse) reflection and the interface (specular) reflection, which is independent of wavelength. The spectral reflectance (radiance factor) $Y(\theta_i, \theta_r, \lambda)$ of the skin surface is a function of the wavelength and the geometric parameters of incidence angle θ_i and viewing angle θ_r. The assumption means that the reflectance is expressed as a linear combination of the diffuse reflectance and the constant reflectance as

$$Y(\theta_i, \theta_r, \lambda) = C_1(\theta_i, \theta_r) S(\lambda) + C_2(\theta_i, \theta_r), \tag{4}$$

where the weights $C_1(\theta_i, \theta_r)$ and $C_2(\theta_i, \theta_r)$ are the geometric scale factors.

We test the adequacy of the standard dichromatic reflection model for the present skin surfaces. To perform this, the PCA analysis is applied to the whole set of spectral reflectance curves observed under different geometries of θ_i and θ_r. Assume that each spectral reflectance is sampled at n points with an equal interval $\Delta\lambda$ (say 5 nm) in the range (400–700 nm). Let $\mathbf{y}(\theta_i, \theta_r)$ and $\mathbf{s}$ be n-dimensional column vectors, representing the observed reflectance $Y(\theta_i, \theta_r, \lambda)$ and the diffuse reflectance $S(\lambda)$, respectively. A singular value decomposition (SVD) of the set of $\mathbf{y}(\theta_i, \theta_r)$ provides that each observed reflectance can uniquely be expressed in a linear combination of the n orthogonal vectors as

$$\mathbf{y}(\theta_i,\theta_r) = \mu_1 v_1(\theta_i,\theta_r)\mathbf{u}_1 + \mu_2 v_2(\theta_i,\theta_r)\mathbf{u}_2 + \ \ldots$$
$$+ \mu_n v_n(\theta_i,\theta_r)\mathbf{u}_n = k_1(\theta_i,\theta_r)\mathbf{u}_1 + k_2(\theta_i,\theta_r)\mathbf{u}_2 + \ \ldots$$
$$+ k_n(\theta_i,\theta_r)\mathbf{u}_n. \qquad (5)$$

where $\{\mu_1,\mu_2,\ldots,\mu_n(\mu_i>\mu_{i+1})\}$, are the singular values of the observation matrix of all $\mathbf{y}(\theta_i,\theta_r)$, $\{\mathbf{u}_1,\mathbf{u}_1\ldots,\mathbf{u}_n\}$, are the left singular vectors, and $\{v_1(\theta_i,\theta_r),v_2(\theta_i,\theta_r),\ldots,v_n(\theta_i,\theta_r)\}$, are determined from the right singular values. A computer program for SVD is given by Press et al.[13] Consider an approximate representation of the reflectances in terms of some component vectors chosen from $\mathbf{u}_1,\mathbf{u}_2,\ldots,\mathbf{u}_n$, The performance index of the chosen principle components is given by the percent variance $P(K)=\Sigma_{i=1}^{K}\mu_i^2/\Sigma_{i=1}^{n}\mu_i^2$.

The above SVD technique is used for testing the standard dichromatic reflection model.[4] The procedure for testing the two assumptions of two-dimensionality and constant reflectance is described as follows:

(1) For the first assumption, we examine whether all the observed reflectances are represented by only first two component vectors $\mathbf{u}_1$ and $\mathbf{u}_2$.
(2) The second test is to determine whether the constant spectrum is described by the two components $\mathbf{u}_1$ and $\mathbf{u}_2$. That is, we examine the validity of a unit vector $\mathbf{i}=a\mathbf{u}_1+b\mathbf{u}_2$ with suitable weights a and b.

The reflectances of IKD-54 were measured at 81 viewing angles of −80°, −78°,…, −2°, 0°, 2°,…, 78°, 80° and 13 incidence angles of 0°, 5°, 10°,…, 60°. First, a 61×1053 reflectance matrix was constructed by sampling the spectral curves at 5 nm intervals. Second, 61 singular vectors $\mathbf{u}_1,\mathbf{u}_2,\ldots,\mathbf{u}_{61}$, were obtained from SVD. The performance index then became $P(1)=0.9960$ and $P(2)=0.9999$. Therefore, it was determined that the spectral reflectances are two-dimensional, which means that they can be described by only the two component vectors $\mathbf{u}_1$ and $\mathbf{u}_2$. Third, the vectors $\mathbf{u}_1$ and $\mathbf{u}_2$ were fit to the unit vector $\mathbf{i}$ using linear regression. Figure 7 shows the fitting result, where the broken straight line and the red curve represent, respectively, the constant spectrum $\mathbf{i}$ and the curve fitted by $\hat{\mathbf{i}}=\hat{a}\mathbf{u}_1+\hat{b}\mathbf{u}_2$. The constant spectrum is estimated as a spectral component of the data set. In Fig. 7, the blue curve represents the direct measurement $\mathbf{s}$ of the diffuse reflectance $S(\lambda)$. All curves are normalized as $\|\mathbf{i}\|^2=\|\hat{\mathbf{i}}\|^2=\|\mathbf{s}\|^2=1$. For the above two reasons, we conclude that the spectral reflectance of the skin surface has the property of standard dichromatic reflection.

Synthesis

Let us consider the estimation of spectral reflectances for various angles of incidence and viewing without observation. The constant reflectance i and the diffuse reflectance $S(\lambda)$ are used to represent the observed reflectances with sufficient accuracy. So it is expected that we can represent any unknown reflectance in terms of the same two component curves. The estimate can be expressed as a function of two parameters in the form

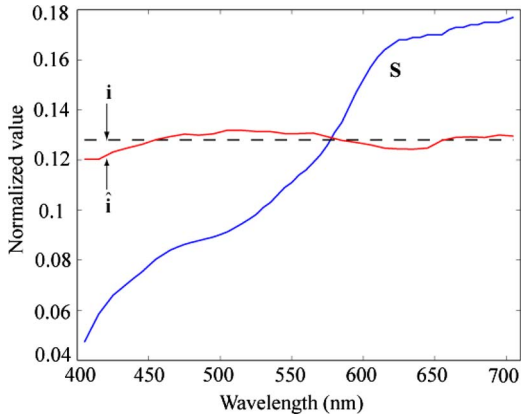

Figure 7. Test of the standard dichroic reflection model for IKD-54. The broken straight line and the red curve represent, respectively, the constant spectrum $\mathbf{i}$ and the curve fitted by $\hat{\mathbf{i}}=\hat{a}\mathbf{u}_1+\hat{b}\mathbf{u}_2$. The blue curve represents the direct measurement $\mathbf{s}$ of the diffuse reflectance $S(\lambda)$.

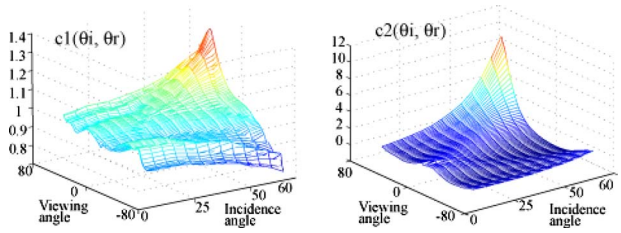

Figure 8. Distributions of the coefficients obtained from the measurements of IKD-54.

$$Y(\theta_i,\theta_r,\lambda) = \hat{C}_1(\theta_i,\theta_r)S(\lambda) + \hat{C}_2(\theta_i,\theta_r), \qquad (6)$$

where $\hat{C}_1(\theta_i,\theta_r)$ and $\hat{C}_2(\theta_i,\theta_r)$ denote the estimates of the weighting coefficients at a pair of angles (θ_i,θ_r).

In order to develop the estimation procedure, we analyze the weighting coefficients based on the observed data. Figure 8 shows the distributions of the coefficients $C_1(\theta_i,\theta_r)$ and $C_2(\theta_i,\theta_r)$ obtained from the measurements of IKD-54. Note that the diffuse coefficient C_1 varies in a limited range [0.8, 1.4], while the specular coefficient C_2 increases steeply when the angles of incidence and viewing become large.

Because each of the weighting coefficients has a two-dimensional distribution in the domain of $0\le\theta_i\le60$ and $-80\le\theta_r\le80$, we can represent the distribution by a matrix $\mathbf{C}$, where the column and the row correspond to θ_i and θ_r. When SVD is applied to the matrix, $\mathbf{C}$ is expanded into two sets of the orthonormal vectors $\{\mathbf{w}_i\}$ and $\{\mathbf{v}_i\}$ $(i=1,2)$ on column and row as $\mathbf{C}=\mathbf{w}_1\mathbf{v}_1^t+\mathbf{w}_2\mathbf{v}_2^t$, where $\{\mathbf{w}_i\}$ are the principal components on the incident angle θ_i and $\{\mathbf{v}_i\}$ are the principal components on the viewing angle θ_r. Therefore, mathematically, the weighting coefficients C_1 and C_2 can be expressed by two basis functions with a single parameter as

$$C(\theta_i,\theta_r) = w_{11}(\theta_i)v_{11}(\theta_r) + w_{12}(\theta_i)v_{12}(\theta_r),$$

$$C_2(\theta_i,\theta_r) = w_{21}(\theta_i)v_{21}(\theta_r) + w_{22}(\theta_i)v_{22}(\theta_r). \qquad (7)$$

Figure 9 shows two sets of principal component curves (v_{11},v_{12}) and (v_{21},v_{22}) as a function of viewing angle θ_r. The

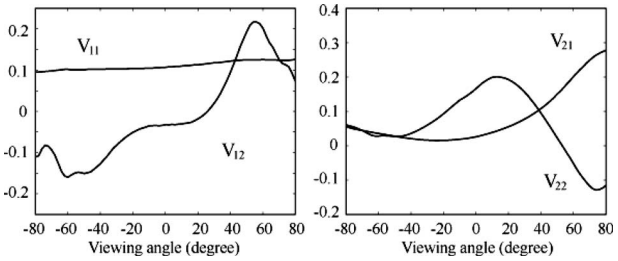

Figure 9. Principal component curves (v_{11}, v_{12}) and (v_{21}, v_{22}) for IKD-54 as a function of viewing angle.

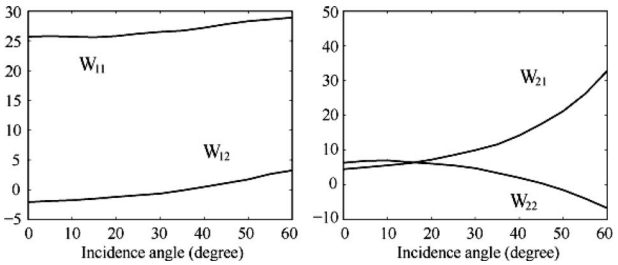

Figure 10. Weights (w_{11}, w_{12}) and (w_{21}, w_{22}) for IKD-54 as a function of incidence angle.

performance indices on IKD-54 are P(1)=0.9956 and P(2)=0.9962 for C_1 and P(1)=0.8778 and P(2)=0.9739 for C_2. The weights (w_{11}, w_{12}) and (w_{21}, w_{22}) for these principal component curves are depicted as a function of incidence angle θ_i in Figure 10. The same SVD computation is done on each of the other samples listed in Table I.

Therefore, the estimation of $\hat{C}_1(\theta_i, \theta_r)$ and $\hat{C}_2(\theta_i, \theta_r)$ for any unknown reflectance can be reduced into a simple form

$$\hat{C}_1(\theta_i, \theta_r) = \hat{w}_{11}(\theta_i)v_{11}(\theta_r) + \hat{w}_{12}(\theta_i)v_{12}(\theta_r),$$

$$\hat{C}_2(\theta_i, \theta_r) = \hat{w}_{21}(\theta_i)v_{21}(\theta_r) + \hat{w}_{22}(\theta_i)v_{22}(\theta_r), \qquad (8)$$

where $\hat{w}_{ij}(\theta_i)$ $(i,j=1,2)$ are determined by interpolating the coefficients at observation points such as $w_{ij}(0)$, $w_{ij}(5), \ldots, w_{ij}(60)$, Thus, the spectral reflectance of the skin surface at arbitrary angular conditions is generated using the diffuse spectral reflectance $S(\lambda)$, two pairs of the principal component weights $v_{ij}(\theta_r)$ $(i,j=1,2)$, and two pairs of weights $w_{ij}(\theta_i)$ $(i,j=1,2)$. It should be noted that these basis data are all one-dimensional.

EXPERIMENTAL RESULTS

The feasibility of the proposed PCA-based method is examined for estimating the surface-spectral reflectance of foundation samples with different material compositions. The surface-spectral reflectance of each sample was measured at 13 incidence angles and 81 viewing angles by the goniospectrophotometer. First, the diffuse spectral reflectance $S(\lambda)$ was determined from the average of the measured reflectances with low radiance and without specularity among 1053 reflectance measurements. Figure 11 depicts the spectral curves of diffuse reflectance for the six samples. Second, the principal components of the spectral reflectances were extracted from SVD of the reflectance data. The adequacy of the standard dichromatic reflection model was then tested on the principal components. The performance indices for the first two components are $P(2)>0.9999$ for all samples. It was found that all the samples satisfied the conditions of standard dichromatic reflection. Third, the two-dimensional coefficient data (C_1, C_2) were further decomposed into the components v_{ij} and w_{ij} $(i,j=1,2)$ based on viewing and incidence angles using SVD.

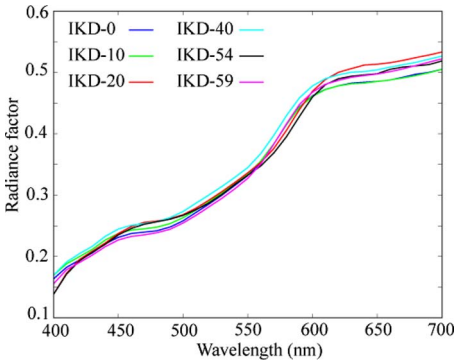

Figure 11. Spectral curves of diffuse reflectance for foundation samples.

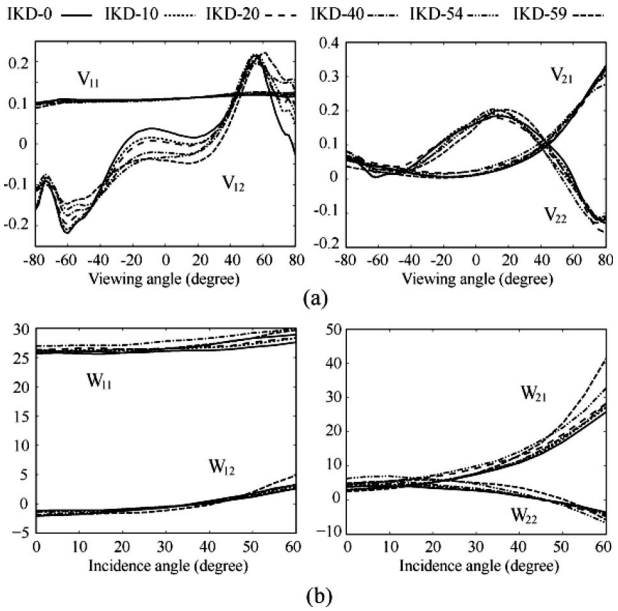

Figure 12. Whole sets of the principal components (v_{11}, v_{12}), (v_{21}, v_{22}) and the weights (w_{11}, w_{12}), (w_{21}, w_{22}) obtained for all samples.

Figure 12 summarizes the whole set of principal components (v_{11}, v_{12}), (v_{21}, v_{22}) and the weights (w_{11}, w_{12}), (w_{21}, w_{22}) obtained for all samples, which includes the curves for IKD-54. Note that the second principal component v_{12} of the diffuse coefficient C_1 represents mainly the reflectance difference among different materials when the viewing angle changes. Finally, the diffuse reflectance $S(\lambda)$, the principal components v_{ij}, and the weights w_{ij} were synthesized to estimate the skin surface-spectral reflectance $Y(\theta_i, \theta_r, \lambda)$ at arbitrary incidence and viewing directions. The unknown weighting coefficients without measurements were estimated by interpolating the known coefficients with a smooth curve obtained from measurements at 13 different incident angles and 81 different viewing angles.

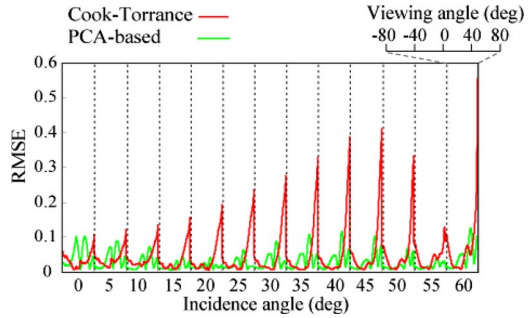

Figure 13. RMSE of the estimated spectral reflectances at every incidence angle and every viewing angle.

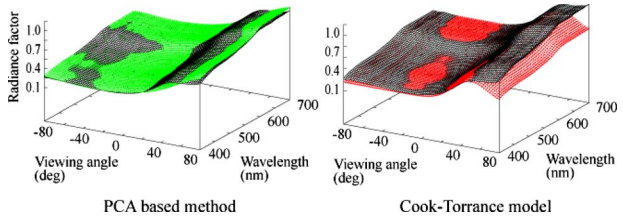

Figure 14. Typical estimation results for surface-spectral reflectance for IKD-54 at the incidence angle of 45°. The color meshes of black, red, and green indicate, respectively, the original measurement, the Cook-Torrance model, and the proposed method.

Figure 13 shows the root-mean-squared error (RMSE) of the estimated spectral reflectance at every incidence angle and every viewing angle, where green curves represent the errors by the proposed method and, for comparison, the red curves represent the errors by the Cook-Torrance model. A comparison between the two curves suggests that the proposed method performs more precise reflectance estimation at most angles of incidence and viewing than the Cook-Torrance model, except for angles close to the angles of normal incidence and viewing.

Figure 14 shows the typical estimation results of surface-spectral reflectance for IKD-54 at the incidence angle of 45°. The black mesh in each figure indicates the original measurements, and the red mesh in the right figure indicates the fitting results by the Cook-Torrance model. The green mesh indicates the estimates by the proposed method, which were obtained from only the reflectance curve in Fig. 7 and the coefficient data in Figs. 9 and 10. We note that the estimated reflectances are almost coincident with the measurements at all viewing angles, while clear discrepancy occurs for the Cook-Torrance model at large viewing angles. For numerical evaluation, we calculated numerical difference and colorimetric error between the estimated reflectances and the direct measurements. Table III lists the RMSE and the CIE 1976 color differences under CIE D65 for all foundation samples.

In order to confirm the estimation accuracy for reflectance without measurement, a simulation was performed in the following two steps. First, by assuming that the spectral reflectances at one incident angle are unknown, we exclude the one from the original data set. Next, we reproduce the eliminated spectral reflectance curves at all viewing angles from the remaining reflectance data at 12 incident angles.

Table III. Root mean squared errors and CIE 1976 color difference for all foundation samples.

	RMSE		ΔE^*ab	
Samples	Cook-Torrance	PCA	Cook-Torrance	PCA
IKD-0	0.053	0.021	2.73	1.24
IKD-10	0.059	0.023	2.94	1.32
IKD-20	0.073	0.024	3.90	2.03
IKD-40	0.070	0.030	3.21	1.62
IKD-54	0.089	0.039	4.38	2.52
IKD-59	0.071	0.043	2.93	2.12

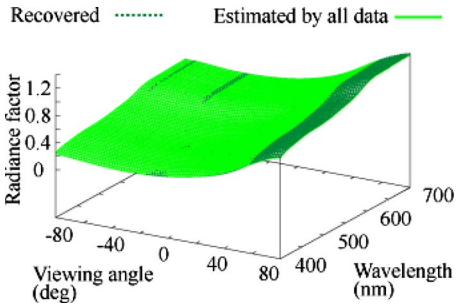

Figure 15. Comparison between the recovered curves from the remaining data and the estimated curves from all data for IKD-54 at 45°. The dark green dotted mesh and the light green solid mesh indicate, respectively, the recovered curves and the estimated curves from all data by PCA.

Table IV. Color differences between the rendered images by the estimated reflectances and the ones by the measurements.

Viewing angle (deg)	ΔE^*ab	
	Cook-Torrance	PCA
–20	1.341	2.383
–10	1.782	3.020
0	2.427	3.266
10	3.095	3.049
20	3.160	2.034
30	2.942	2.182
40	3.325	4.469
50	4.479	4.235
60	6.943	1.983
70	12.759	2.977
80	18.435	2.989

Then, the accuracy is examined by comparison among the neglected measured curves, the curves recovered from the remaining data, and the estimated curves from all data by PCA. Figure 15 shows the comparison for IKD-54 at 45°. The dark green mesh with dotted curves indicates the recovered curves from the remaining reflectance data. The light green mesh with solid curves indicates the estimated curves

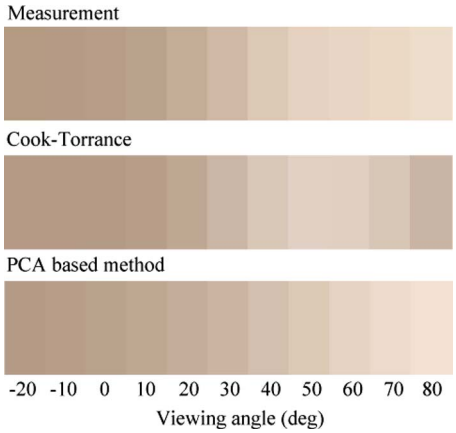

Figure 16. Color images of skin surface with IKD-54 at different viewing angles.

Figure 17. Rendered images of a human hand with different make-up foundations.

from all data, which are the same curves as shown in the left of Fig. 14. Two meshes are almost perfectly coincident. Thus, any unknown reflectance without observation is adequately estimated.

Figure 16 demonstrates color images rendering the appearance of skin surface with IKD-54 under different viewing angles. We assume that the surface is illuminated from the direction of incidence 45° with CIE D65. Table IV lists the color differences between the rendered images by the estimated reflectances and the ones by the measurements for all color patches. The proposed method provides more accurate color reproduction, especially at large viewing angles, compared with the Cook-Torrance model.

For application to image rendering, we rendered color images of the skin surface of a human hand using the estimated reflectances. The 3D shape of a human hand was acquired using a laser range finder system. Figure 17 demonstrates the rendered images of the 3D skin surface with different make-up foundations. A ray-tracing algorithm was used for rendering realistic images, which performed wavelength-based color calculation precisely. The light source is D65, and the incidence angle is 10°.

CONCLUSION

This article has analyzed the spectral reflection properties of skin surface with make-up foundation. Foundations with different material compositions were painted on a bioskin. First, we measured the spectral reflectance of the skin surfaces under a variety of conditions of light incidence and viewing. Second, we showed the limitations of the model-based approach for describing the complicated reflectance curves by a small number of parameters. Third, a new approach based on PCA was proposed for describing the detailed shape of the surface-spectral reflectance function. All skin surfaces have the property of standard dichromatic reflection, so that the observed reflectances can be expressed as a linear combination of two spectral components of constant reflectance and diffuse reflectance. Moreover, we have found that the weighting coefficients are decomposed into two basis functions with a single parameter. As a result, the spectral reflectance under arbitrary observation conditions can be estimated by synthesizing the diffuse spectral reflectance and several one-dimensional basis functions. Finally, the feasibility of the proposed method was examined using foundation samples. The PCA-based approach can provide reliable estimates of the spectral reflectances from a global point of view. Color images using the estimated spectral reflectances demonstrated the appearance of skin surfaces. The authors will continue to make an effort to improve the estimation accuracy of the PCA-based method.

ACKNOWLEDGMENT

The authors would like to thank Kanebo Cosmetics for providing the samples of cosmetic foundation and supporting this work.

REFERENCES

[1] E. Angelopoulou, R. Molana, and K. Danilidis, "Multispectral skin color modeling", *Proc. IEEE Conference of Computer Vision and Pattern Recognition* (IEEE, Piscataway, NJ, 2001), pp. 635–642.
[2] N. Tsumura, N. Ojima, K. Sato, M. Shiraishi, H. Shimizu, H. Nabeshima, S. Akazaki, K. Hori, and Y. Miyake, "Image-based skin color and texture analysis/synthesis by extracting hemoglobin and melanin information in the skin", ACM Trans. Graph. **22**, 770–779 (2003).
[3] M. Doi, N. Tanaka, and S. Tominaga, "Spectral reflectance estimation of human skin and its application to image rendering", J. Imaging Sci. Technol. **49**, 474–482 (2005).
[4] P. Boré, *Cosmetic Analysis: Selective Methods and Techniques* (Marcel Dekker, New York, 1985).
[5] S. Tominaga and Y. Moriuchi, "PCA-based reflectance analysis/synthesis of cosmetic foundation", *Proc. IS&T/SID's 16th Color Imaging Conference* (IS&T, Springfield, VA, 2008), pp. 195–200.
[6] B. T. Phong, "Illumination for computer-generated pictures", Commun. ACM **18**, 311–317 (1975).
[7] R. Cook and K. Torrance, "A reflection model for computer graphics", *Proc. SIGGRAPH 81* (ACM, New York, 1981), Vol. **15**, pp. 307–316.
[8] S. Tominaga and S. Nishi, "Surface reflection properties of oil paints under various conditions", Proc. SPIE **6807**, 0M1–0M8 (2008).
[9] K. E. Torrance and E. M. Sparrow, "Theory for off-specular reflection from roughened surfaces", J. Opt. Soc. Am. **57**, 1105–1114 (1967).
[10] M. Born and E. Wolf, *Principles of Optics* (Pergamon Press, Oxford, UK, 1987), pp. 36–51.
[11] R. Hall, *Illumination and Color in Computer-Generated Imagery* (Springer-Verlag, Berlin, 1989).
[12] S. Tominaga and B. Wandell, "Standard reflectance model and illuminant estimation", J. Opt. Soc. Am. A **6**, 576–584 (1989).
[13] W. H. Press, S. A. Teukolsky, W. T. Vetterling, and B. P. Flannery, *Numerical Recipes in CC+* (Cambridge University Press, Cambridge, UK, 2002).